Analysis of Mechanical Analog for Understanding ACL Injuries

Caitlin O'Dea, Rebecca Cree, and Carl Faust[a)]

Department of Physics, Susquehanna University, 514 University Ave., Selinsgrove, Pennsylvania 17870, USA

[a)] Corresponding author: faust@susqu.edu

Abstract. We present an experimental study of a mechanical system intended to approximate a situation in which an anterior cruciate ligament (ACL) injury could occur during a collision between soccer players. To stand in for a collision force, increasing weight pulled on a "leg" analog system. Weight was added until one of two situations occurred: the soccer cleat came loose from the turf, corresponding to a slip, or a spring in the "knee" compressed past a given threshold, corresponding to an ACL injury. Data from these tests were analyzed using a simple statics model, and conclusions can be drawn about how parameters such as height, weight, cleat type, and collision force contribute to the likelihood of an ACL injury.

INTRODUCTION

Many introductory physics classes designed for nonphysics majors are populated with students interested in professions in the biological or medical fields. Making motivating connections between concepts like force, momentum, and energy to biological systems can often be challenging, especially in laboratory settings [1]. The literature has a wide range of examples of demonstrations, lab experiments, and lecture content aimed at addressing this potential disconnect [2]. Examples with connections to human and wildlife anatomy and physiology, sports, or medical injuries can often be very effective, as they provide real-world, concrete scenarios that students often have direct experience with [3,4]. Work by Plomer et al. highlights the benefits of incorporating physiologically based experiments on medical students' understanding and attitudes toward physics [5]. These motivating labs and demonstrations often aim to help students understand a potentially complex biological system by simplifying relevant concepts and experimental analyses so that connections to the physical models are more apparent. For example, Yang and Kim analyze the jumping of elastic steel hoops as an analogy for the jumping mechanism in the bodies of various types of insects [6].

The system analyzed in this work focuses on injuries of the anterior cruciate ligament (ACL). The ACL is the central ligament of the knee that is responsible for minimizing lateral and rotational movement. Two primary mechanisms of ACL injuries are when a soccer cleat is planted into the ground and (1) there is a quick change of motion or (2) the athlete experiences a lateral hit from another player as illustrated in Fig. 1(a) [7,8]. These injuries are typically more common in female soccer players [9], and when an athlete tears this ligament, they must undergo surgery and 9–12 months of physical therapy to return to their sport [10].

This work focuses on understanding incidents where an athlete's foot is planted and a collision occurs. Multiple factors contribute to whether an incident like this results in an ACL tear. Parameters such as the design of the cleat, height and weight of the athlete, strength of the ACL, and playing surface all contribute to the effective grip strength of the player's feet. Several studies have investigated different types of turf, including those that have small rubber infill pellets, and how they affect grip strength and potentially lead to injuries [11–13]. The two styles of soccer cleats in our experiment are round-studded cleats and angled-studded cleats. The former has azimuthally symmetric studs, and the latter is studded with an apparent preferred directionality.

Understanding how the different parameters affect the possibility of an ACL injury not only allows athletes to make informed decisions when choosing cleats, but also provides engaging insights to students interested in studying medical sciences. A variety of factors can contribute to an ACL injury, and making use of a simplified system can provide fundamental insight into how and why these injuries might occur and what factors separate a dangerous scenario from a safe one. This paper will present a description of the apparatus acting as the mechanical analog for the ACL, a theoretical analysis of the system, experimental data and results, key takeaways from the results, and concluding remarks.

EXPERIMENTAL DESCRIPTION

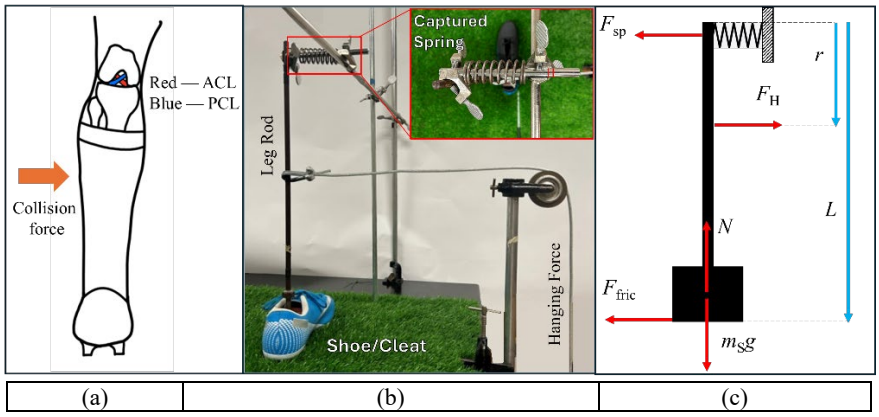

FIGURE 1. (a) Rear view of a left leg in a potential collision scenario with highlighted ACL and posterior cruciate ligament, PCL. (b) ACL analog leg system with inset that shows a closeup of the captured spring. (c) A free-body diagram showing the forces acting on the leg rod.

The primary experimental method involves investigating forces acting on a simplified mechanical analog of the ACL/leg/cleat system, shown in Fig. 1(b). Using standard lab rods and clamps, a structure that acts as a support for the leg system is fixed to a lab table covered in soccer turf material. The leg system consists of two main parts: the cleat and the ACL analog. The shoe is attached to the bottom of the vertical leg rod via washers and nuts on either side of a hole drilled into the cleat. The cleat is oriented to be pulled from the side to create the most realistic representation of an ACL injury that would occur from a collision or lateral force on the lower leg.

The ACL analog, shown in the inset of Fig. 1(b), consists of a 90-degree joint clamp attached at the top of the leg rod. This clamp holds a smaller rod that passes through the center of a strong spring. The other end of this smaller rod passes through a second 90-degree joint clamp on the table rod structure. The second clamp is closed just enough so that the small rod is held in position but still allowed to move freely within the clamp. This results in the spring being captured between the two clamps. When the leg rod is pulled toward the table rod structure, the small rod passes further through the clamp and causes the spring to compress. The compression force of the spring is analogous to that exerted on the ACL during a collision.

The collision force is represented by a cable pulling horizontally on the leg rod. The cable passes over a pulley so weights can be hung to vary the force. The pulley can be raised and lowered to maintain a horizontal direction when the collision position along the leg rod is changed. For all these tests, the cleat was oriented on the turf so the horizontal force pulled sideways toward the inner side of the shoe. This roughly corresponds to a collision that impacts the outer side of the leg as depicted in Fig. 1(a), which represents a likely scenario for an ACL injury [8].

Data was obtained with the force of the hanging mass acting at three different heights along the 0.53-meter leg rod. Measured from the top of the leg rod, the heights 0.05 m, 0.23 m, and 0.41 m were marked and referred to as knee, shin, and ankle, respectively. At each height, mass was incrementally added to the cleat, representing a player's weight. For each amount of mass in the shoe m_S, weight was added to the pulley to increase the horizontal force on the leg rod. The hanging mass was increased until one of two thresholds was reached. Either the cleats slipped along the turf by a specific threshold distance or the spring compressed by a specific threshold length. The former case, deemed "safe," corresponds to a scenario where a player loses their footing, slips, and falls due to the collision. The latter case, deemed "dangerous," corresponds to a scenario where the impact force causes damage to the ACL.

Note that although we analyze the safe case using only standard static friction, in a practical sense, the cleat's horizontal grip strength includes contributions from static friction as well as other forces associated with the cleat studs digging into the turf. When the cleat's studs become embedded in the ground or turf, this additional horizontal surface force can raise the limiting value required for the cleat to slip. On turf fields, small rubber infill pellets are often used to increase grip strength, which can vary with infill density and piling up [12,13]. Despite these additional forces, there will still be a maximum limiting value, so we analyze this case using static friction and consider μ_S to be the effective coefficient of static friction that accounts for all forces contributing to the grip strength. This value would likely be higher than the standard value of the coefficient of static friction between two flat-surfaced materials.

In the safe and the dangerous scenarios, both the cleat friction and the spring forces are nonzero. However, one of these forces will reach its threshold values first, allowing us to label each data point as either safe or dangerous. The threshold cleat slip distance (about 0.5 cm) and the threshold spring compression length (about 1 cm) were consistent for all measurements, and both were chosen based on practical considerations and to ensure that the data spanned a range illustrative of the various possible scenarios. For example, if the threshold length for spring compression was too large (analogous to an extremely strong ACL), most or all data points obtainable with the available masses would result in safe scenarios. The ranges of forces and weights available for this experiment were too small to replicate those found in a realistic scenario.

For each shoe mass and collision location, the hanging mass required to reach a threshold was determined. To do this, hanging mass was first added in large increments to overshoot the breaking point and obtain an upper limit. Weight was then removed and readded in smaller increments to approach the breaking point more precisely. The most suitable small increment masses were 100 g. As a result, this represents the amount of precision in our measurements of the collision force. Weight was added slowly and carefully to maintain precision and repeatability, and for safety, to prevent any sudden kicks. Each collision force measurement was labeled as safe or dangerous depending on which threshold was reached first.

STATICS ANALYSIS OF LEG SYSTEM

To model the results we might expect to see from this experiment, we analyzed the system as a simple statics problem. Figure 1(b) shows the free-body diagram for the system. Three forces are important: the spring force F_{sp}, which can take values between zero and kx_0; the static friction force F_{fric}, which can take values between zero and $\mu_S m_S g$; and the horizontal external force due to the hanging mass F_{H}. The origin for the distance along the leg is taken at the top of the leg rod; however, the position of the axis of rotation is taken to be at the top or bottom of the leg rod for analyzing the safe case and dangerous case, respectively. By choosing the axis of rotation at these locations, the unknown torque located at $r = 0$ is eliminated from the statics analysis and we are only left with a relationship between F_{H} and the force which has reached its threshold.

In the safe case, the static friction force will reach its limiting value before the spring force. We can determine the predicted value of the required horizontal force by setting the net torque equal to zero when the static friction reaches its critical point:

$$\Sigma\tau = \tau_{\text{sp}} + \tau_{\text{H}} + \tau_{\text{fric}} + \tau_N + \tau_{mg} = 0. \tag{1}$$

The torques due to the weight and normal force are zero, since the forces are parallel to the leg rod. In the safe case, we will take the axis of rotation to be at the top of the rod, which results in $\tau_{\text{sp}} = 0$. Plugging in the torque from the horizontal force and friction, we get $rF_{\text{H}} - L\mu_S m_S g = 0$, where r is the distance from the top and L is the length of the leg rod as seen in Fig. 1(b). When solving for the hanging force we find that

$$F_{\text{H}} = \frac{L\mu_S m_S g}{r}. \tag{2}$$

Although the value of the spring force was not measured for safe cases, we can also determine its value at the threshold by setting the net force in the horizontal direction equal to zero, $\Sigma F_x = F_{\text{H}} - F_{\text{sp}} - F_{\text{fric}} = 0$. Plugging in values for the horizontal force and friction force at the threshold for the safe case gives $F_{\text{sp}} = \left(\frac{L}{r} - 1\right)\mu_{\text{s}} m_{\text{s}} g$.

In the dangerous case, the spring force will reach its limiting value before the static friction force. Similar to the safe case, we can use the net torque in Eq. (1) to predict the horizontal force required to reach this limit. For this case, we take the axis of rotation to be at the bottom of the leg rod, which results in $\tau_{\text{fric}} = 0$. After plugging in expressions for the horizontal torque and spring torque we get $Lkx_0 - (L - r)F_{\text{H}} = 0$, giving us

$$F_{\text{H}} = \frac{Lkx_0}{L - r}. \tag{3}$$

Again, for completeness, we can also find the value of the friction force, even though this was not measured for dangerous cases. Setting the net force in the horizontal direction equal to zero and plugging in values for the spring and horizontal forces we find that $F_{\text{fric}} = \left(\frac{L}{L-r}\right) kx_0$.

Equations (2) and (3) describe what we should expect to find as the horizontal force required to reach the relevant threshold in the safe and dangerous cases. For the safe case, the horizontal force increases linearly with the mass in the shoe. This continues until the spring force reaches its threshold, after which the horizontal force required stays constant with mass in the shoe. The amount of mass in the shoe that serves as the transition point can be found by setting Eqs. (2) and (3) equal to solve for m_{C}, the cutoff mass:

$$m_{\text{C}} = \left(\frac{r}{L-r}\right)\frac{kx_0}{\mu_S g}. \tag{4}$$

This model, although simplified, describes many of the variables that account for whether a particular collision on a soccer field will be dangerous in terms of an ACL injury. Length L corresponds to the length from foot to knee and is likely proportional to a player's height, while the mass in the shoe m_S corresponds to a player's weight. The value r describes the location of the collision on the leg, kx_0 is an estimate of the strength of the ACL, and μ_S is the effective coefficient of static friction. Recall that the coefficient of static friction is a combination of static friction and additional horizontal forces generated by the cleats digging into the turf and the turf infill pushing back against the studs.

DATA AND RESULTS

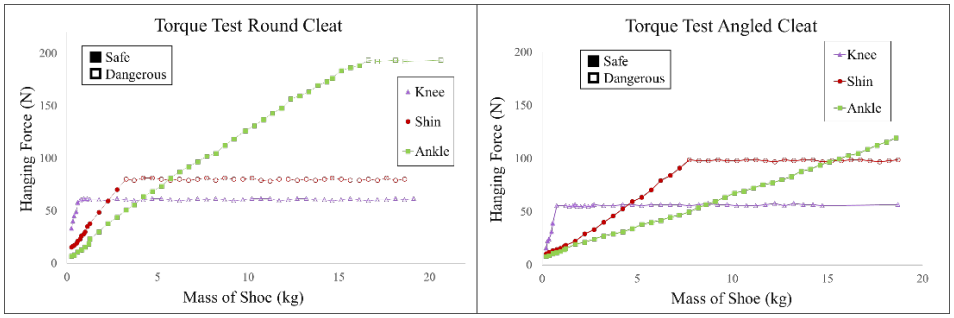

(a) (b)

FIGURE 2. Plots of the angled-cleat (a) and round-cleat (b) torque test. Solid points represent safe scenarios where the cleat slips on the turf by a threshold distance, and the hollow points represent dangerous scenarios where the spring compresses a threshold distance. Each color/shape represents a different location for the horizontal hanging force along the leg rod.

Figure 2 shows data obtained for the horizontal hanging force described. The solid data points indicate where the cleat slipped first. These data increase linearly with increasing mass in the shoe, as expected in the safe-case theory [Eq. (2)]. The hollow data points indicate where the spring compressed past its threshold distance first. These points are relatively constant with increasing mass in the shoe, as expected in the dangerous case theory [Eq. (3)].

Several interesting features can be noted from the data in Fig. 2. First, the structure of the plots in the low- and high-end limiting cases for mass of the shoe follow what we might expect intuitively. A low mass in the shoe would roughly correspond to a situation with a relatively lightweight player. A collision along the lower leg would be more likely to cause the player to lose footing and be tripped; however, the collision force needed to cause this trip would increase further up the leg (knee > shin > ankle). A large mass in the shoe would correspond to a situation with a relatively heavyweight player. The heavier weight produces a stronger grip between the cleat and the ground, keeping the player's feet planted. A collision in this scenario is more likely to injure the ACL, or knee in general. However, in this case the same severity of injury would require a larger collision force further down the leg, in a trend opposite to that of the low mass in the shoe (ankle > shin > knee).

While both limiting cases are rather intuitive, the data in between these regions, where the cases transition, show a feature that may not be immediately intuitive. The slanted trapezoid-shaped region describes a set of masses where the shin can take more collision force than either the knee or the ankle before slipping or causing injury. In this region, a collision on the knee would lead to an ACL injury when an otherwise identical collision at the ankle would instead cause a slip.

Other important takeaways include the impact of effective friction (or grip strength) and the spring compression force (or ACL strength) on the collision force required for either case. As previously mentioned, several factors contribute to a cleat's grip strength in addition to static friction; however, considering these as part of the total effective friction reveals its effect on the data. In general, a stronger grip strength means that larger forces are required to cause slipping, resulting in steeper slopes in the safe-case regions. Since the horizontal force required to slip increases more quickly with mass on the shoe, a dangerous scenario can occur for lower-mass situations. By wearing cleats that have a strong grip via friction, stud size, stud placement, and turf interaction, players are more likely to experience a scenario that results in ACL injury, even if they are lighter and might otherwise be tripped by a collision. From the data in Fig. 2, we find that the slopes in the case of round cleats were steeper than the case of angled cleats, implying that for a sideways collision, wearing rounded cleats means players have greater potential for ACL injuries. When determining which style of soccer cleat to purchase, athletes have to decide whether to prioritize performance or safety. Cleats designed for better performance provide a strong grip and allow the athlete to make quick and abrupt direction changes. Cleats that prioritize safety still allow athletes to play soccer as usual but with less grip, to reduce the risk of injury.

The spring compression force was kept constant in this experiment but could have been varied by choosing a smaller or larger value of x_0, corresponding to a weaker or stronger ACL, respectively. Increasing the ACL strength would result in higher constant values in the dangerous regions, meaning that stronger collisions would still cause the cleat to slip before an ACL injury occurs.

In addition to this work, we also used Eqs. (2) and (3) to estimate the friction coefficients and spring constant of the system, and then we compared them to separate, independent measurements. Furthermore, we found that cleats with angled studs offer more friction front-to-back than side-to-side, enabling safer scenarios with side-on collisions while still maintaining a stronger forward grip. These results and further discussion of some of the practical limitations of this experiment are detailed in the Appendix.

CONCLUSION

The experiment presented here aims to help students identify and quantify the effects of a variety of parameters that might influence the likelihood of a soccer collision injuring a player's ACL. These parameters include player attributes such as height and weight; collision factors like impact location, force, and ACL strength; and grip, which accounts for cleat type, friction, and other factors that contribute to the grip strength acquired by digging into the ground or turf. The data show that angled studs are safer during a side-on collision due to less overall side-to-side grip. The simple mechanical apparatus and model identify general trends related to these parameters as well as quantify values analogous to grip and ACL strength. Many avenues could be expanded upon to develop a more robust model in future work. Scaling the parameters to values comparable to human-scale weight, height, and ACL strength would provide a more direct measurement of these trends. Also, the horizontal force used to represent the collision force was added slowly and incrementally. Modifying the experiment to allow the hanging weight to be dropped to simulate a sudden impact might reveal the effect of collision speed on injury risk. Finally, this experiment focused on a collision force as the catalyst for the injury. Many other ACL injuries are caused by sudden pivots or rotations along an axis going parallel to the leg [13]. Although incorporating these additional factors might require further complexity in the model, the straightforward analogy between real-life factors and the mechanical analogs presented here offers a unique way for players to develop a general intuition about what is important to consider when seeking to avoid ACL injuries on the field.

REFERENCES

1. G. Kortemeyer, "The challenge of teaching introductory physics to premedical students," *Phys. Teach.* **45**, 552–557 (2007).
2. M. J. Madsen, "Physics myth busting: A lab-centered course for non-science students," Phys. Teach. **49**, 448–451 (2011).
3. D. Liu and Z. Duan, "Simulations of back and arms," Phys. Teach. **59**, 544–546 (2021).
4. D. G. Haase, "Football physics: The science of the game: Timothy Gay," Phys. Teach. **43**(7), 480 (2005).
5. M. Plomer, K. Jessen, G. Rangelov, and M. Meyer, "Teaching physics in a physiological meaningful manner," Phys. Rev. ST-PER. **6**, 020116 (2010).
6. E. Yang and H.-Y. Kim, "Jumping hoops," Am. J. Phys. **80**, 19–23 (2012).
7. P. Renstrom, A. Ljungqvist, E. Arendt, B. Beynnon, T. Fukubayashi, W. Garrett, T. Georgoulis, T. E. Hewitt, R. Johnson, T. Krosshaug, et al., "Non-contact ACL injuries in female athletes: An International Olympic Committee current concepts statement," Br. J. Sports Med. **42**, 394–412 (2008).
8. J. G. Betts, K. A. Young, and J. A. Wise, Anatomy of selected synovial joints, in *Anatomy and Physiology 2e* (OpenStax, 2022), pp. 340–341.
9. Holly Silvers-Granelli, "Why female athletes injure their ACL's more frequently," Int. J. Sports Phys. Ther. **16**, 971–977 (2021).
10. A. M. Kiapour and M. Murray, "Basic science of anterior cruciate ligament injury and repair," NLM **3**, 20–31 (2014).
11. M. Ngatuvai, "Epidemiological comparison of ACL injuries on different playing surfaces in high school football and soccer," NLM **10** (2022).
12. S. Forrester and P. Fleming, "Traction forces generated during studded boot-surface interactions on third-generation artificial turf: A novel mechanistic perspective," Eng. Rep. **1**(5) (2019).
13. Melissa M. Mansfield and Ronald B. Bucinell. Effects of playing surface and shoe type on ACL tears in soccer players, Am. J. Eng. App. Sci. **9**(4), 1150–1157 (2016).

APPENDIX

Additional Experimental Analysis and Discussion

Although this method involved directly measuring the horizontal force versus mass in the cleat, applying the model given by Eqs. (2) and (3) allows us to analyze the data to estimate values for other parameters, including the effective coefficient of friction μ_S and the spring constant k. To check the estimates of these parameters, we first performed separate independent measurements to obtain comparison values. To find the effective coefficient of static friction for both cleat types, mass was incrementally added to the shoe, which was placed flat on the turf by itself (separate from the rest of the torque test apparatus). The same pulley setup was used to find the amount of hanging mass that caused the cleat to slip. To keep the setup as consistent as possible with the torque test parameters, we used the same threshold slipping distance and measuring method to determine whether the cleat had moved. When plotting the hanging mass required versus the mass in the cleat and applying a linear fit, the slope gives the effective coefficient of static friction under the same conditions as those in the torque test. Although, as mentioned, the torque test was performed with the horizontal force pulling toward the inner side of the cleat, we also found the effective coefficients of static friction by pulling the cleat from the back. Figure 3(a) shows the data from these tests along with the coefficients obtained from the linear fits. A notable result from these tests is the difference in the coefficients for the angled cleats when pulled sideways versus backward. From the image of the cleat bottoms in Fig. 3(b), we might expect this difference, as the studs on the angled cleats have a clear directionality that results in a preferred orientation, while the studs on the rounded cleats have azimuthal symmetry. The difference in friction for the angled cleats also highlights that the overall grip strength of the cleats incorporates contributions from factors other than just the friction between two surfaces.

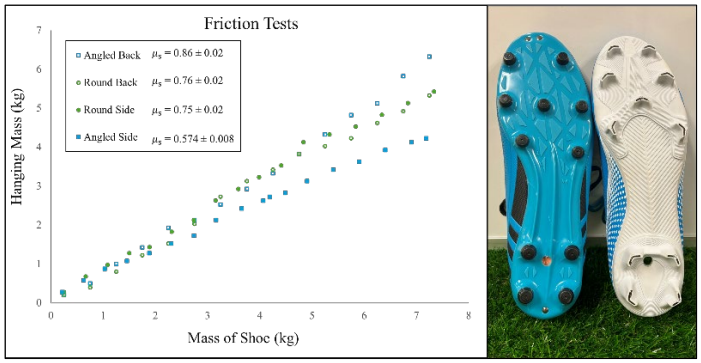

(a) (b)

FIGURE 3. (a) Data for the independent horizontal friction test for both cleat types in two different directions. (b) Bottom view of cleats showing rounded (left) and angled (right) stud shape and arrangements

To obtain an estimate of the effective coefficients of friction for each cleat type from the torque test, we considered the safe-case data in Fig. 2. Each set of sloped safe data can be described by Eq. (2), so by comparing a linear fit of each set of sloped data to Eq. (2), we find "Slope" $= \frac{L\mu_S g}{r}$.

By plotting these slopes versus $1/r$, shown in Fig. 4, and applying a linear fit, the "slope of slopes" should be equal to $L\mu_S g$, allowing us to solve for the effective friction coefficient μ_S from the known values of L and g for both the angled and round cleats; see Table 1.

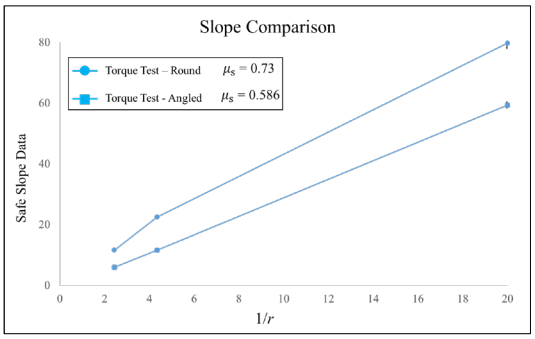

FIGURE 4. The slopes obtained from "safe" data were used to determine effective friction coefficients for each cleat type.

Similar to the friction coefficient, we obtained an independent measurement of the spring constant k. This was done by simply stacking masses on top of the spring and recording the spring's length for each. Figure 5 shows the weight of the stacked masses plotted versus the spring's length change and fitted linearly to obtain a value of the spring constant. To estimate this value from the torque test data, we consider the dangerous case data in Fig. 2, which is described by Eq. (3). Since the data for the dangerous case should not depend on the mass in the cleat or the friction resulting from the cleat type itself, all data points corresponding to dangerous cases can be grouped together by calculating $F_H \times (L - r)$ for each. According to Eq. (3), these values should correspond to Lkx_0, from which we can determine an average value of k from known values of L and x_0.

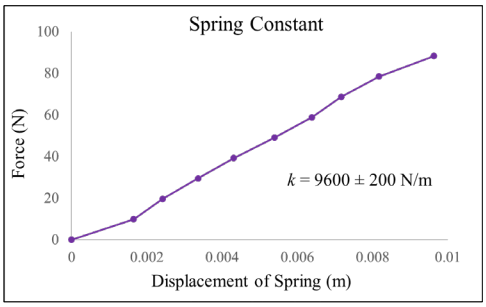

FIGURE 5. Data for the independent measurement of the spring constant for the spring used to represent the ACL.

Table 1 displays the comparisons between independent measurements of the coefficients of friction and spring constant and the values obtained from the torque test data. Each of these values agrees to within one or two standard deviations. Although independent measurements of these values might be more precise and straightforward to obtain, the values obtained from analyzing torque test data highlight the broad range of details that can be determined from this method. These data also suggest a general conclusion that although round cleats might be less effective than angled cleats at providing grip for forward motion, they seem to have stronger grip than angled cleats in a sideways direction, which could be undesirable in a potential side-collision ACL scenario.

TABLE 1. Comparison of values for the effective friction coefficient and the spring constant based on data collected from the ACL torque test and separate independent measurements of each quantity.

	Effective Friction Coefficient	
	Horizontal Friction Test	ACL Torque Test ("Safe" Slope)
Angled Cleat	0.574 ± 0.008	0.586 ± 0.002
Round Cleat	0.75 ± 0.02	0.73 ± 0.04
	Spring Constant (N/m)	
Angled and Round Cleat	Spring Constant Test	ACL Torque Test (Average "Dangerous" Data)
	9600 ± 200	10,300 ± 900

While the torque test experiment follows a relatively straightforward procedure, there are several practical factors that must be addressed, or at least considered, when drawing conclusions about how the data might describe a real-life ACL injury scenario. Most significantly, the amount of mass available for the cleat and horizontal force presented both a limit to the range of data that could be explored as well as physical considerations about where and how to secure masses and the continual matting of the turf texture. The largest mass data point taken at the ankle on the round cleat required around 40 kg total, split between the hanging mass and the cleat mass. To accommodate this range of mass, additional support rods were used to stabilize the structure attached to the table, and a steel cable was used to connect the cleat with the hanging mass. Even if more mass were available and could be supported structurally, securing additional mass to the cleat would take up more space, which would be difficult without stacking masses further up the leg rod. We also sought to ensure that mass in the cleat was generally evenly distributed so that all cleat studs remained in contact with the turf. We cut inserts from a sheet of lead to make "heavy insoles," which provided an even distribution of mass, efficient use of space, and a flat surface on which to place other masses. Despite all of these solutions, as shown in Fig. 2, no dangerous case data were obtained for the ankle with the angled cleat. Using Eq. (4) to estimate the cutoff mass in the cleat for this case, we might expect approximately 36 kg on the cleat and 19 kg as the hanging mass, which were not available nor practical for this work.